Journal of Alloys and Compounds 520 (2012) 272–276

Contents lists available at SciVerse ScienceDirect

Journal of Alloys and Compounds

journal homepage: www.elsevier.com/locate/jallcom

Effect of temperature on the exchange bias in naturally oxidized Ni_xCo_{1-x} ($x = 0.2$) nanowires fabricated by electrochemical deposition technique

K. Maaz[a,c], Soo Hyun Kim[b], Myung-Hwa Jung[b], Gil-Ho Kim[a,*]

[a] Department of Electronics and Electrical Engineering and Sungkyunkwan University Advanced Institute of Nanotechnology (SAINT), Sungkyunkwan University, Suwon 440-746, Republic of Korea
[b] Department of Physics, Sogang University, Seoul 121-742, Republic of Korea
[c] Nanomaterials Research Group, Physics Division, PINSTECH, Nilore, Islamabad, Pakistan

ARTICLE INFO

Article history:
Received 22 November 2011
Received in revised form
21 December 2011
Accepted 7 January 2012
Available online 15 January 2012

PACS:
75.70Rf
75.50Gg
75.50Tt

Keywords:
Polycrystalline
Electrodeposition
Exchange bias

ABSTRACT

Ni_xCo_{1-x} ($x = 0.2$) nanowires (with controlled diameter and length of ~120 nm and 30 μm) have been fabricated by electrochemical deposition. Oxide layer of ~6 nm has been developed over a period of 400 days by natural oxidation of the wires. Temperature dependent magnetic analysis shows an increasing behavior of coercivity with decreasing temperature while field cooled hysteresis curves $M(H)$ show exchange bias effect and vertical shift in magnetization below 150 K. This study demonstrates that the nanowires constitute *core–shell* cylindrical structure with ferromagnetic cores surrounded by antiferromagnetic oxide shells, which show blocking temperature of 150 K much lower than the Neel temperature of bulk Ni- and Co-oxide.

1. Introduction

In recent years most of the research has been focused on magnetic nanowires (NWs) fabricated by electrochemical deposition technique [1]. For spintronic applications it is very important to combine desirable properties of two or more materials into one-dimensional structures like the nanowires. In these structures various phases of magnetic materials (e.g. metal and metal oxide) are distributed in layers in the radial direction along the core–shell geometry at the nanoscale. In this regime when one or more dimensions are reduced to the order of domain wall length or exchange length, magnetic properties become strongly dependent on structural geometry of the materials. In such materials the surface spins play crucial role as far as their magnetic properties are concerned. These spins cause, for example, reduction in saturation magnetization (Ms), enhancement in coercivity (H_c), or the appearance of exchange bias at low temperatures. The surface spins do not exactly follow the core anisotropy direction and become disordered or canted leading to the formation of magnetically bilayer system with different magnetic anisotropies. In case of metallic nanowires the outer layers are generally made of their oxides, which are magnetically antiferromagnetic (AFM) while the inner layers are metallic, which are ferromagnetic (FM) in nature. Formation of oxide layers at the surface of nanowires take place as a result of the natural oxidation of metallic cores of the wires at the atmospheric conditions.

In template embedded NWs the templates provide protection against the rapid oxidation of the wires thereby decreasing the oxidation rate at the outer surfaces. Thickness of oxide layer usually depends on the nature of polymer–wire interface. As polycarbonate (PC) is permeable to atmospheric oxygen therefore oxidation occurs at the interface of the wires and the templates [2]. In case of 30 nm diameter cobalt NWs an average oxide layer of ~4 nm has been measured after a delay time of about 800 days [3]. While in case of Co thin films (>5 nm) about 2.5 nm thick oxide layer has been reported [4]. The development of AFM oxide layer in general causes loss of magnetic properties in the wires; however, this can also give the possibility of effectively tuning magnetic properties at the interface of two magnetic media. This is done by modifying the oxidation layer thickness, which is of special interest for the application of these nanowires in spintronic devices, whereas the metal and the metal–oxide structures are of special interest due to their spin-dependent quantum transport properties.

* Corresponding author. Tel.: +82 31 290 7989; fax: +82 31 299 4618.
E-mail address: ghkim@skku.edu (G.-H. Kim).

0925-8388/$ – see front matter © 2012 Elsevier B.V. All rights reserved.
doi:10.1016/j.jallcom.2012.01.040

Temperature dependent magnetic analysis in multilayered systems leads to several interesting phenomena including the exchange bias (H_{ex}) effect [5,6]. The exchange coupling at FM–AFM interface may induce unidirectional anisotropy in FM materials, below the Neel temperature of AFM, shifting the loop along the field axis [6]. H_{ex} has also been observed in other bilayer systems involving ferromagnetic, ferrimagnetic, and spin glass (SG) like materials [5,6]. This phenomenon has been investigated mainly in thin films and nanoparticles [7–9]. However, this effect has been recently observed in nanowires as well [10,11]. In this case there exists a well defined hard and easy axis of magnetization due to their strong shape anisotropy, especially in cylindrical nanowires that play a crucial role in determining both magnitude and direction of H_{ex} in such systems. Competition between the shape and field cooled induced anisotropies can be tailored to study magnetic properties and exchange bias effect in these nanowires.

In this work, nickel–cobalt NWs with controlled diameters (120 nm) have been fabricated by electrochemical deposition in porous polycarbonate membranes. The wires have been naturally oxidized over a period of about 400 days at an oxide layer of thickness ~6 nm. Temperature dependent magnetic properties have been studied in detail and the results have been explained in terms of the recent models with reference to core–shell interactions at FM–AFM interface and the surface effects causing temperature dependent variations in magnetic properties in these nanowires.

2. Experimental procedure

Polycarbonate membranes were used as the hosting materials for fabrication of nanowires. These templates were obtained by swift heavy ion irradiation (i.e. specific energy 11.4 MeV/nucleon) of 30 μm thick PC foils. The foils were subsequently etched in an aqueous solution of 5 M NaOH with an etching rate of 2 μm h^{-1}. Diameter of the pores (120 nm) was controlled by the etching-time during the etching process while length of the wires was fixed (30 μm). The working electrode was then deposited on one side of the membrane by DC sputtering (<10 nm Au) and then strengthened by electrochemical deposition of Cu (~5 μm thick) layer. The membrane was then clamped in a holder that was exposed to the electrochemical bath on the porous side (~1 cm^2 area), allowing the solution to penetrate into the pores of the membranes. The electrolyte consists of one molar solution of cobalt and nickel sulfates (added with a ratio of ~8:2) with pH of the solution was adjusted to 6 by adding appropriate amount of H_2SO_4. The deposition was carried out at constant voltage of −1 V at room temperature. Further details are given in the previous work [12]. Morphology of the wires was investigated by high resolution transmission electron microscopy (HRTEM), while the composition was studied by dispersive spectroscopy (EDS) and elemental mapping techniques. For analyzing texture of the wires X-ray diffraction (XRD) technique was used. Moreover, magnetic characterization was performed by SQUID-magnetometer up to ±20 kOe field. For SQUID analysis the measurements were carried out with wires embedded in polycarbonate templates. The direction of the applied field in SQUID analysis was kept parallel to the wire long axis (longitudinal measurements). For TEM analysis the nanowires were liberated from the templates by dissolving it in dichloromethane (CH_2Cl_2) while for XRD analyses the wires were left embedded in the templates.

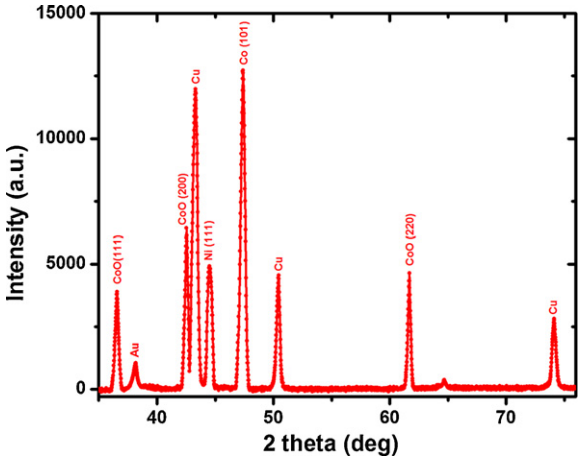

Fig. 1. X-ray diffraction pattern of $Ni_{0.2}Co_{0.8}$ NWs oxidized for ~400 days. The peaks in the pattern are indexed for Ni, Co, and CoO according to standard JCPDF cards mentioned in the text.

3. Results and discussion

Fig. 1 shows the XRD pattern of the nanowires that exhibits main reflections at [1 0 1], [1 1 1], and [2 0 0], which are describable for hcp Co, fcc Ni, and fcc CoO, respectively. These peaks are indexed according to JCPDF cards 89-4308, 87-0712, and 74-2392 for these materials. The extra peaks in the pattern correspond to Au and Cu used as the sputtered and substrate materials. Fig. 2 shows a representative TEM images of the wires, which were liberated from the templates by dissolving in di-chloromethane. The inset table of Fig. 2(a) obtained from the EDS analysis provides the quantitative presence of various elements constituting these nanowires. It is seen in Fig. 2(a) that the diameter of the wires is about 120 nm while the EDS analysis shows that about ~5% oxygen atoms are present in the wires most probably at the surface of the wires in the form of Co- and/or Ni-oxide. To further explore the oxide layer thickness around the nanowires a high resolution TEM image is shown in Fig. 2(b). The oxide layer of 6 nm thickness surrounding the core of the wires as seen in the figure is composed of polycrystalline CoO and/or NiO. The labeled distance of ~0.192 nm

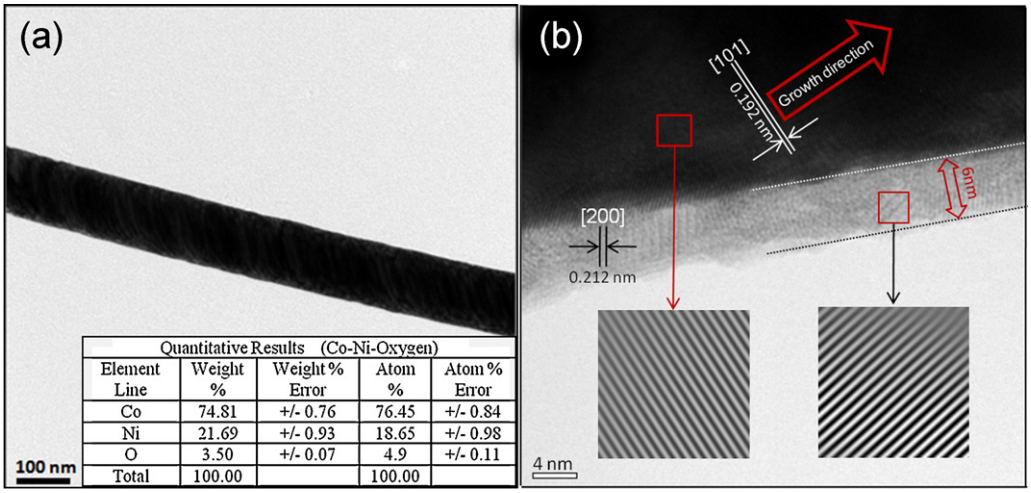

Fig. 2. TEM image of (a) oxidized NWs with a diameter of ~120 nm liberated from the templates, with inset table represents the EDS results, and (b) the wires indicating 6 nm polycrystalline CoO/NiO shell constituting around the core of the wires.

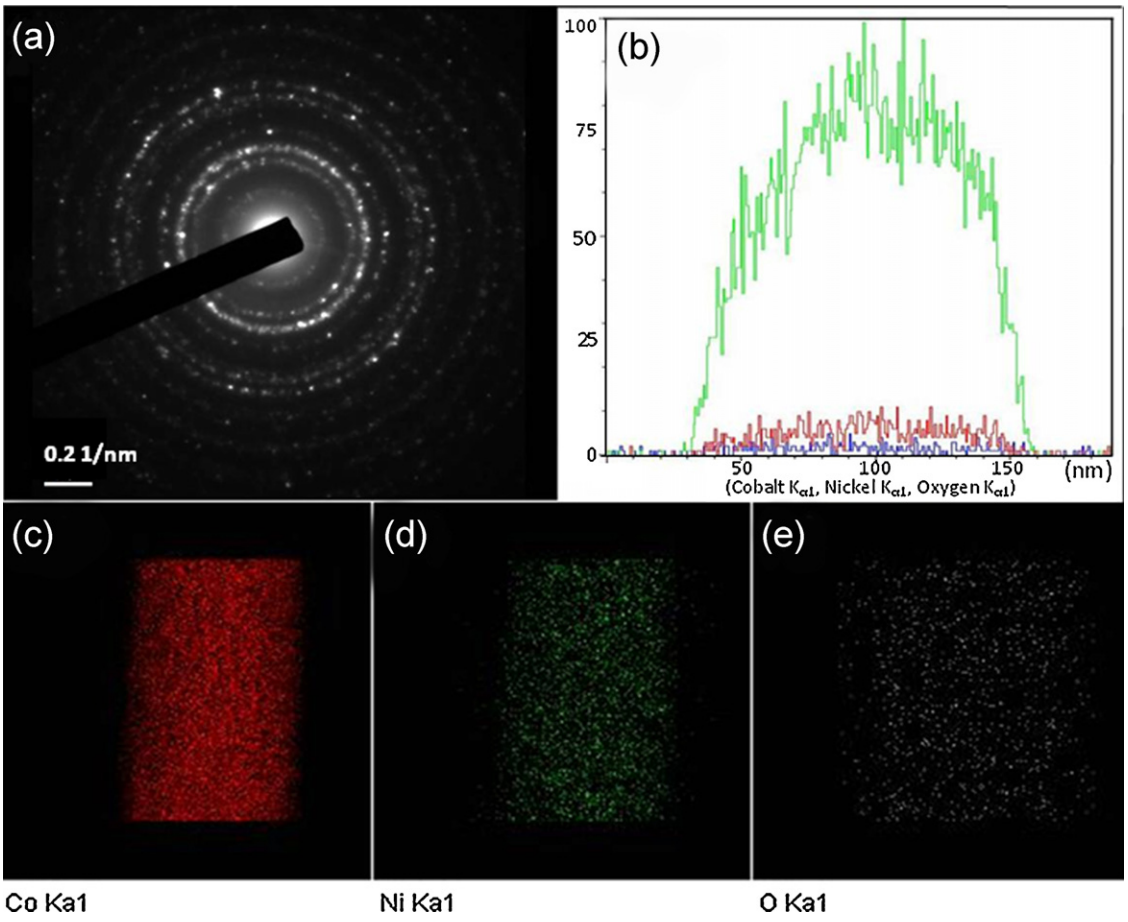

Fig. 3. (a) SAED pattern of NWs, which confirms poly-crystallinity of the wires. (b) Elemental mapping of $Ni_{0.2}Co_{0.8}$ NWs, which indicates the relative intensities of Co, Ni, and oxygen present in the nanowires, (c) indicates the relative concentration of metallic cobalt, (d) nickel, and (e) oxygen in the nanowires. (For interpretation of the references to color in the text, the reader is referred to the web version of the article.)

corresponds to (1 0 1) plane for hcp cobalt while the inter planner distance of ~0.212 nm corresponds to (2 0 0) plane for fcc CoO according to the JCPDF cards mentioned above. The arrow shown in Fig. 2(b) represents the growth direction in the nanowires. Fig. 3(a) shows the SAED pattern obtained from a segment of a wire that reveals the polycrystalline nature of these NWs. In order to further explore the distribution of cobalt, nickel, and oxygen in the oxidized $Ni_{0.2}Co_{0.8}$ NWs, elemental mapping was achieved for a segment of nanowire as shown in Fig. 3(b)–(e). The colors shown in the figure indicate the relative concentration of Co, Ni, and oxygen within a diameter of ~120 nm. These concentrations are shown separately in Fig. 3(c)–(d) as the Co, Ni, and oxygen constituting the nanowires.

Magnetic characterization of the nanowires was performed by SQUID magnetometer. The measurements were made from 3 K to 300 K under an applied field of ±20 kOe. Fig. 4 shows the field cooled (FC) $M(H)$ loops taken at various temperatures from 3 to 300 K under ±20 kOe with inset of the figure represents the expanded region for the visibility of the readers. Fig. 5 shows the temperature dependence of zero field cooled (ZFC) and FC coercivities which show increasing trends with decreasing T. In Fig. 5 it is to be noticed that below ~150 K called the blocking temperature (T_B) or the effective Neel temperature (T_N) of nanostructured AFM shell the FC H_c shows an increasing trend as compared to ZFC H_c and this becomes more significant as T decreases further. The blocking temperature of the wires at 150 K has also been deducted from $M(T)$ curves shown in the inset of Fig. 5, which represents a clear bifurcation of FC and ZFC curves at $T_B \approx 150$ K.

To discuss the increasing behavior of H_c at lower temperatures it is believed that the strong intrinsic temperature dependent anisotropy of FM core plays crucial role in these nanowires. If we consider thermal fluctuations in polycrystalline nanowires then H_c can be written as [1,13,14];

$$H_{c(T)} = H_0(T)\left[1 - \left(\frac{25k_BT}{KV}\right)^{1/m}\right] \quad (1)$$

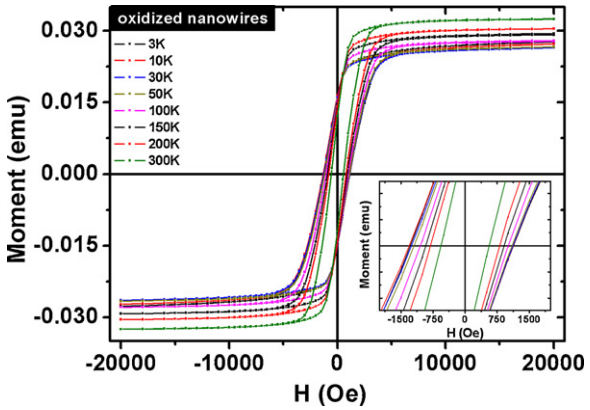

Fig. 4. Temperature dependent $M(H)$ loops of oxidized $Ni_{0.2}Co_{0.8}$ NWs at 3, 10, 30, 50, 100, 150, 200, and 300 K. The inset represents the magnified region for the visibility of the readers.

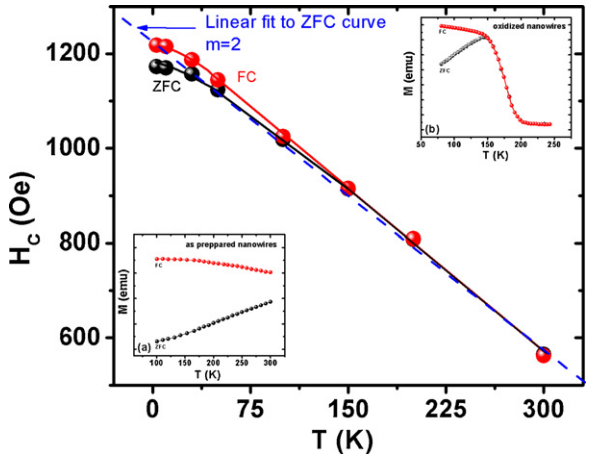

Fig. 5. Temperature variation of H_c with red line shows the FC H_c while the black line indicates the ZFC H_c. The dotted line shows the fit curve to ZFC coercivity according to Eq. (1) with $m = 1$ The two insets represent the $M(T)$ curves for the oxidized and fresh nanowires.

where $H_0(T)$ is the zero-temperature coercivity, k_B is the Boltzmann constant, K is the anisotropy energy density, which is of the order of 10^6 erg/cm^3 for nanocrystalline cobalt at room temperature, and V is the volume of each magnetic switching domain, respectively. It is noticeable that the value K for cobalt oxide is larger due to an additional AFM phase present in the core/shell NWs. Referring back to Fig. 5, the blue line shows the fit curve to ZFC H_c according to Eq. (1) using T as the fitting parameter. As evident from Fig. 5 the data fits very well to the above relation with $m = 2$. Thus the simple model of thermal activation of moments is applicable for our core–shell nanowires. At temperatures below ~20 K, there seems some deviation from the above relation that cannot be simply interpreted by thermal activation model. There may be other contributions from the inter-wire dipolar interactions, or the SG-like behavior of the shells. Since the density of nanowires is low (~10^8 wire/cm^2) that approximates the inter-wire distance of ~450 nm, which is two high than the exchange length (l_{ex}) of 3.4 and 9.9 nm for cobalt and nickel respectively. Therefore the possibility of inter-wire interactions can be excluded; however the SG-like phase can play the role at reduced temperatures.

At T below 20 K the AFM shell spins can freeze into their random sates (SG phase) enabling the shell to prevent the core spins to further respond to the applied field. This may result into the saturation of FC and ZFC coercivities and causes the deviation from the thermal activation model similar to the case of core/shell ferrite nanoparticles [15]. As discussed earlier the departure (increase) of FC H_c form ZFC H_c below 150 K shown in the inset (b) of Fig. 5 is attributed to the presence of AFM shell composed of CoO and NiO. This causes an additional contribution to the anisotropy of the system at T_B much smaller than T_N of bulk CoO/NiO, which in turn increases the FC H_c of the wires below this temperature [16]. Fig. 6 shows the FC $M(H)$ loops of the as-prepared $Ni_{0.2}Co_{0.8}$ NWs to compare their magnetic properties with oxidized wires and to explore the effect of oxide layer on exchange bias and blocking temperature of system. In Fig. 6 it is seen the $M(H)$ loops are symmetric about the origin in the whole temperature range indicating no exchange bias below 150 K. This suggests that this effect is originated in the core/shell NWs due to its oxidized nature. Furthermore, to explore the effect of oxide layer on T_B we refer to the $M(T)$ curves of the as-prepared nanowires shown in the inset (b) of Fig. 5. We see that there is no overlap between the two curves even at 300 K, suggesting that the as-prepared Ni/Co NWs are in ferromagnetic state in the whole temperature range of our measurements.

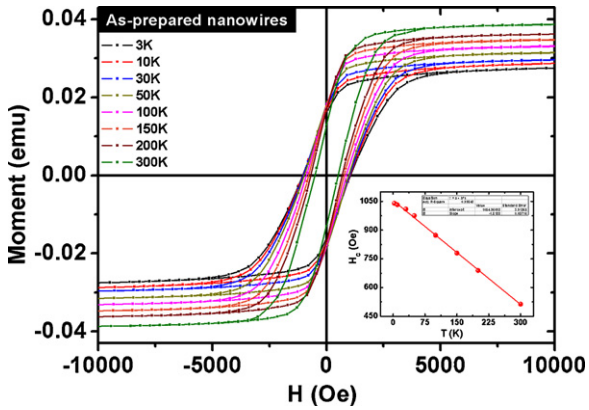

Fig. 6. Temperature variation of FC H_c for the as-prepared nanowires with fit curve to the data.

Fig. 7 shows H_{ex} as a function of T with interesting behavior that it disappears above 150 K, while below this temperature H_{ex} increases almost linearly to 3 K. This negligible H_{ex} above 150 K is due to the oxide shell that loses its AFM order by reaching its T_B (effective Neel temperature) much lower than T_N for bulk CoO/NiO [16]. The observed T_N, lower than the bulk value of CoO/NiO, is due to the 6 nm thick AFM shell (see Fig. 2) where the finite size effects can play the dominant role. When the shell thickness is smaller than certain system dependent critical dimensions of the outer layer, the T_B is substantially reduced from the bulk value [16]. It has been reported that in case of high quality thin films with thicker AFM layers $T_B \approx T_N$, while in case of polycrystalline thin films with AFM shells (of few nm) like in our case T_B is much smaller than T_N [17]. Thus at 150 K H_{ex} vanishes in the samples, which in good agreement with previous reports for similar core/shell Co/CoO nanoclusters and nanoparticles at 150 K [18,19]. The increase of H_{ex} below T_B (Fig. 7) can be explained in light of the same argument that explains the variation of H_c with temperature, i.e. the application of thermal activation model to these nanowires as discussed earlier.

Fig. 7 shows δM as a function of temperature which shows that δM is zero above 150 K while it is maximum (~7×10^5 emu) at ~150 K, and then decreases with decreasing temperature to ~3 K. The positive shift of δM in our case indicates the positive spins interactions at the interface between the two magnetic media (FM core and AFM shell). The presence of vertical shift accompanying the exchange bias is generally associated with uncompensated pinned spins present at the core–shell interface [9]. We assume that in case

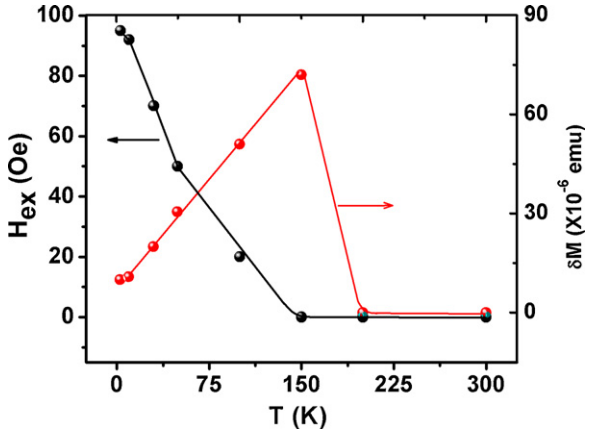

Fig. 7. Variation of H_{ex} (black curve) as a function of temperature of NWs. The red curve shows δM as a function of temperature.

of core/shell nanowires the high temperatures enable more of the interfacial spins to become decoupled from the AFM shell and be pinned with the interface in the direction close to the applied field, thereby increasing the vertical shift at 150 K, similar to the case of core/shell nanoparticles reported earlier [9].

4. Conclusion

In this work polycrystalline core–shell Ni_xCo_{1-x} ($x = 0.2$) nanowires have been fabricated by electrochemical deposition in PC templates. An oxide layer of ~6 nm has been obtained over a period 400 days due to the natural oxidation of metallic NWs in the atmospheric conditions. Temperature dependent magnetic analyses showed an increasing behavior of H_c with decreasing temperature that has been attributed to the enhancing role of magnetocrystalline anisotropy and diminishing thermal effects in the system. Negligible exchange bias has been found above ~150 K that has been attributed to the oxide layer that loses its AFM order above T_B (effective T_N of nanostructured AFM shell) and is unable to bias the FM core to produce H_{ex} while the decrease of δM with T, below 150 K has been attributed to the interfacial spins that become decoupled from the AFM shell and pinned with core/shell interface in the direction of the applied field.

Acknowledgments

This research was supported by World Class University (WCU) program funded by the Ministry of Education, Science and Technology through the National Research Foundation of Korea (R32-10204).

References

[1] D.J. Sellmyer, M. Zheng, R. Skomsky, J. Phys.: Condens. Matter 13 (2001) R433.
[2] J.C. Salamone, Polymeric Materials Encyclopedia, CRC, Boca Raton, 1996.
[3] J. De La Torre Medina, M. Darques, L. Piraux, J. Appl. Phys. 106 (2009) 023921.
[4] L. Smardz, et al., J. Appl. Phys. 71 (1992) 5199.
[5] J. Nogués, J. Sort, V. Langlais, V. Skumryev, S. Suriñach, J.S. Muñoz, M.D. Baró, Phys. Rep. 422 (2005) 65.
[6] J. Nogués, I.K. Schuller, J. Magn. Magn. Mater. 192 (2009) 203.
[7] C. Tsang, J. Appl. Phys. 55 (1984) 2226.
[8] A. Punnoose, H. Magnone, M.S. Seehra, J. Bonevich, Phys. Rev. B 64 (2001) 174420.
[9] A. Mumtaz, K. Maaz, B. Janjua, S.K. Hasanain, M.F. Bertino, J. Magn. Magn. Mater. 313 (2007) 266.
[10] E.L. Salabas, A. Rumplecker, F. Kleitz, F. Radu, F. Schüth, Nano Lett. 6 (2006) 2977.
[11] J.Y. Yu, S.L. Tang, X.K. Zhang, L. Zhai, Y.G. Shi, Y. Deng, Y.W. Du, Appl. Phys. Lett. 94 (2009) 182506.
[12] K. Maaz, S. Karim, M. Usman, A. Mumtaz, J. Liu, J.L. Duan, M. Maqbool, Nanoscale Res. Lett. 5 (7) (2010) 1111.
[13] J.-H. Gao, Q.-F. Zhan, W. He, D.-L. Sun, Z.-H. Cheng, Appl. Phys. Lett. 86 (2005) 232506.
[14] L.-F. Liu, W.-Y. Zhou, S.-S. Xie, O. Albrecht, K. Nielsch, Chem. Phys. Lett. 466 (2008) 165.
[15] K. Maaz, M. Usman, S. Karim, A. Mumtaz, S.K. Hasanain, M.F. Bertino, J. Appl. Phys. 105 (2009) 113917.
[16] J. Nogues, K. Ivan, Schuller, J. Magn. Magn. Mater. 192 (1999) 203.
[17] J. Nogeus, J. Sort, V. Langlais, V. Skumryev, S. Surinach, J.S. Munoz, M.D. Baro, Phys. Rep. 422 (2005) 65.
[18] K. Sumiyama, T. Hihara, D.L. Peng, R. Katoh, Sci. Technol. Adv. Mater. 6 (2005) 18.
[19] S. Gangopadhyay, G.C. Hadjipanayis, C.M. Sorensen, K.J. Klabunde, Nanostruct. Mater. 1 (1992) 449.